Elastodynamic diffraction by a periodic rough surface (stress-free boundary)

J. T. Fokkema and P. M. van den Berg

Department of Electrical Engineering, Division of Electromagnetic Research, Delft University of Technology, Delft, The Netherlands
(Received 15 June 1977)

The reflection of an elastic wave by a rough stress-free surface with a periodic profile has been investigated rigorously. The problem is formulated in terms of an integral equation for the particle displacement at a single period of the boundary surface. Numerical results pertaining to the reflection of either an incident P wave or an incident SV wave for a sinusoidal profile are presented.

PACS numbers: 43.20.Bi, 43.20.Fn

INTRODUCTION

In this paper the diffraction of elastic waves by a stress-free surface with a periodic profile has been investigated. We present a rigorous theory in which the boundary value problem at the surface is treated by an elastodynamic extension of the Green's function formulation that has been introduced by Lippmann[1] in connection with the scalar theory of reflection gratings.[2] This technique used in the present problem leads to a vectorial integral equation for the unknown particle displacement at a single period of the boundary surface. After a numerical solution, results pertaining to the reflection factors of the different spectral waves are presented. To locate a point in space, we use the Cartesian coordinates x_1, x_2, and x_3. It is assumed that the configuration is independent of x_3. The subscript notation for vectors and tensors will be used. Latin subscripts are to be assigned the values 1, 2, and 3 while Greek subscripts are to be assigned the values 1 and 2; for repeated subscripts the summation convention holds. Occasionally the boldface notation will be used to denote a two-dimensional vector; in particular $\mathbf{x}=(x_1, x_2)$ will denote the two-dimensional position vector.

Throughout the calculations, the complex time factor $\exp(-i\omega t)$, where i denotes the imaginary unit, ω the circular frequency, and t the time, will be omitted in the formulas. (SI units are used throughout.)

I. FORMULATION OF THE PROBLEM AND METHOD OF SOLUTION

A homogeneous, isotropic, perfectly elastic solid occupies a semi-infinite domain with a spatially periodic stress-free boundary Λ (Fig. 1).

The mechanical properties of the material are characterized by its mass density ρ and its stiffness coefficients

$$c_{ijpq}=\lambda\delta_{ij}\delta_{pq}+\mu(\delta_{ip}\delta_{jq}+\delta_{iq}\delta_{jp}), \tag{1}$$

in which λ and μ are the Lamé coefficients of the material and δ_{ij} is the symmetrical unit tensor:

$$\delta_{11}=\delta_{22}=\delta_{33}=1, \quad \delta_{ij}=0 \text{ if } i\neq j.$$

In the medium a two-dimensional wave motion is present, of which the displacement $u_\alpha=u_\alpha(\mathbf{x})$ and the stress $\tau_{\alpha\beta}=\tau_{\alpha\beta}(\mathbf{x})$ satisfy the linearized equation of motion

$$\partial_\beta\tau_{\alpha\beta}+\rho\omega^2u_\alpha=0, \tag{2}$$

and the linearized stress–strain relation

$$\tau_{\alpha\beta}=c_{\alpha\beta\xi\eta}\partial_\xi u_\eta, \tag{3}$$

where ∂_β denotes the partial derivative with respect to x_β.

A uniform, plane wave, having no x_3 dependence is incident upon the boundary Λ of the elastic medium at an angle θ_0 with the negative x_2 axis. Its displacement and stress are written as

$$u^i_\alpha(\mathbf{x})=U^i_\alpha\exp(i\mathbf{k}\cdot\mathbf{x}), \tag{4}$$

$$\tau^i_{\alpha\beta}(\mathbf{x})=T^i_{\alpha\beta}\exp(i\mathbf{k}\cdot\mathbf{x}). \tag{5}$$

This wave is either a compressional wave (P wave) or a vertically polarized shear wave (SV wave). The different quantities associated with the two types of incident waves are listed in Table I. Note that $|U^i_\alpha|=1$. In Table I $\epsilon_{\alpha\gamma}$ denotes the antisymmetrical unit tensor:

$$\epsilon_{11}=\epsilon_{22}=0, \quad \epsilon_{12}=-\epsilon_{21}=1.$$

The elastodynamic quantities of the reflected field are introduced as

$$u^r_\alpha=u_\alpha-u^i_\alpha, \quad \tau^r_{\alpha\beta}=\tau_{\alpha\beta}-\tau^i_{\alpha\beta}, \tag{6}$$

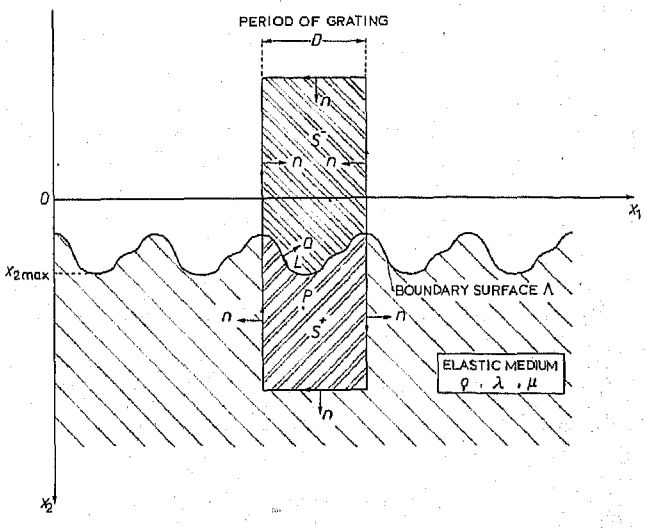

FIG. 1. Periodic configuration and domains to which two-dimensional elastodynamic representation theorems are applied.

TABLE I. Quantities associated with the incident plane wave.

Quantity	Incident P wave	Incident SV wave
Wave number	$k^p = \omega/c_p$	$k^s = \omega/c_s$
Wave speed	$c_p = [(\lambda + 2\mu)/\rho]^{1/2}$	$c_s = (\mu/\rho)^{1/2}$
Wave vector	$\mathbf{k}^p = [k^p \sin(\theta_0^p), -k^p \cos(\theta_0^p)]$	$\mathbf{k}^s = [k^s \sin(\theta_0^s), -k^s \cos(\theta_0^s)]$
U_α^i	k_α^p / k^p	$\epsilon_{\alpha\gamma} k_\gamma^s / k^s$
$T_{\alpha\beta}^i$	$T_{\alpha\beta}^p = i(\lambda k_\gamma^p k_\gamma^p \delta_{\alpha\beta} + 2\mu k_\alpha^p k_\beta^p)/k^p$	$T_{\alpha\beta}^s = i\mu(k_\alpha^s \epsilon_{\beta\gamma} k_\gamma^s + k_\beta^s \epsilon_{\alpha\gamma} k_\gamma^s)/k^s$
Intensity	$\frac{1}{2}\omega^2 \rho c_p$	$\frac{1}{2}\omega^2 \rho c_s$

in which the total stress has to satisfy the boundary condition of the stress-free surface

$$\tau_{\alpha\beta} n_\beta = 0 \quad \text{on } \Lambda , \tag{7}$$

where n_β denotes the unit vector along the outward normal to the boundary. The periodicity of the boundary surface Λ (with period D) entails a quasiperiodicity in the reflected elastodynamic field, viz., $\exp(-ik_1 x_1) u_\alpha^r$ and $\exp(-ik_1 x_1)\tau_{\alpha\beta}^r$ are periodic in x_1. In the domain $x_{2\max} < x_2 < \infty$, where $x_{2\max}$ denotes the maximum value that x_2 can attain on the boundary surface Λ, the reflected elastodynamic field can be written as the superposition of plane waves (both P and SV waves), that are either propagating or exponentially decaying in the positive x_2 direction (the so-called spectral orders).

Let us write the corresponding expression as

$$u_\alpha^r(\mathbf{x}) = \sum_{m=-\infty}^{\infty} \frac{k_{\alpha,m}^p}{k^p} R_m^p \exp(i\mathbf{k}_m^p \cdot \mathbf{x}) + \sum_{m=-\infty}^{\infty} \frac{\epsilon_{\alpha\gamma} k_{\gamma,m}^s}{k^s} R_m^s \exp(i\mathbf{k}_m^s \cdot \mathbf{x}), \quad x_{2\max} < x_2 < \infty , \tag{8}$$

where $\mathbf{k}_m^p = (k_{1,m}^p, k_{2,m}^p)$, $\mathbf{k}_m^s = (k_{1,m}^s, k_{2,m}^s)$, $k_{1,m}^p = k_{1,m}^s = k_{1,m} = k_1 + 2\pi m/D$, $k_{2,m}^p = (k^{p2} - k_{1,m}^2)^{1/2}$, $k_{2,m}^s = (k^{s2} - k_{1,m}^2)^{1/2}$, with $\mathrm{Re}(k_{2,m}^p, k_{2,m}^s) \geq 0$ and $\mathrm{Im}(k_{2,m}^p, k_{2,m}^s) \geq 0$. For the propagating P and SV waves the wave numbers $k_{2,m}^p$ and $k_{2,m}^s$ are real. They are finite in number and for them angles of reflection can be defined, being the angles included between the x_2 axis and the direction of propagation of the wave (cf. Table II and Fig. 2).

Our principal aim is to calculate the reflection factors R_m^p and R_m^s. They follow from a suitable integral representation for u_α^r. The latter is obtained from the two-dimensional form of the elastodynamic representation theorem[3,4] to the domain S^+ inside the closed contour consisting of the straight lines parallel to the x_2 axis, a period D apart, together with the curve L corresponding

TABLE II. Quantities associated with a propagating reflected wave of spectral order m.

Quantity	Reflected P wave	Reflected SV wave
Wave vector	$\mathbf{k}_m^p = [k^p \sin(\theta_m^p), k^p \cos(\theta_m^p)]$	$\mathbf{k}_m^s = [k^s \sin(\theta_m^s), k^s \cos(\theta_m^s)]$
Intensity	$\frac{1}{2}\omega^2 \rho c_p \lvert R_m^p \rvert^2$	$\frac{1}{2}\omega^2 \rho c_s \lvert R_m^s \rvert^2$
Grating formula	$\sin(\theta_m^p) = \sin(\theta_0^p) + 2\pi m/k^p D$	$\sin(\theta_m^s) = \sin(\theta_0^s) + 2\pi m/k^s D$
Snell's law	$k^p \sin(\theta_0^p) = k^s \sin(\theta_0^s)$	

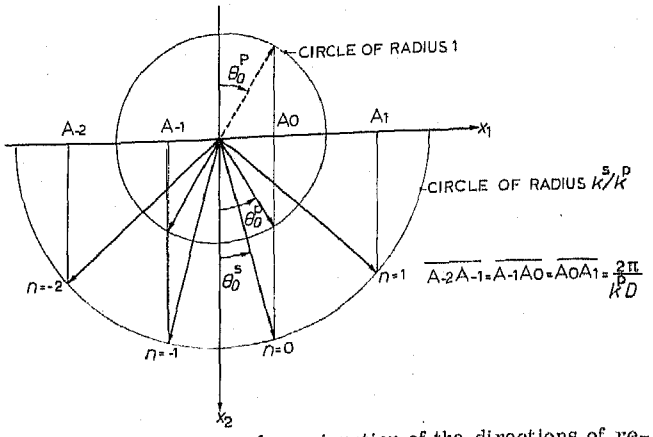

FIG. 2. The geometrical construction of the directions of reflection of the reflected waves (incident P wave, two reflected propagating P waves, and four reflected propagating SV waves) of the different spectral orders from the grating formula and Snell's law, in case of an incident P wave. The modifications in case of an incident SV wave are obvious.

with a single period of the grating profile, and the straight line parallel to the x_1 axis at $x_2 > x_{2\max}$ (see Fig. 1). To carry out this program, we have to employ suitable Green's tensors. For the present case they are straightforward extensions of the scalar Green's function in grating theory[2] to the one for the elastodynamic state.[4] Its displacement $u_{\gamma\alpha}^g = u_{\gamma\alpha}^g(\mathbf{x};\mathbf{x}')$ and its stress $\tau_{\gamma\alpha\beta}^g = \tau_{\gamma\alpha\beta}^g(\mathbf{x};\mathbf{x}')$ are given by

$$u_{\gamma\alpha}^g = (1/\rho\omega^2)[\partial_\gamma' \partial_\alpha' (G^s - G^p) + \delta_{\gamma\alpha} k^{s2} G^s] , \qquad \tau_{\gamma\alpha\beta}^g = c_{\alpha\beta\xi\eta} \partial_\xi' u_{\gamma\eta}^g , \tag{9}$$

where ∂_α' denotes the partial derivative with respect to x_α' and

$$G^p = \sum_{m=-\infty}^{\infty} (i/2k_{2,m}^p D) \exp[ik_{1,m}^p (x_1 - x_1') + ik_{2,m}^p \lvert x_2 - x_2' \rvert] , \qquad G^s = \sum_{m=-\infty}^{\infty} (i/2k_{2,m}^s D) \exp[ik_{1,m}^s (x_1 - x_1') + ik_{2,m}^s \lvert x_2 - x_2' \rvert] . \tag{10}$$

The Green's tensor represents the elastodynamic response to a concentrated force, subject to quasiperiodic boundary conditions at vertical sides parallel to the x_2 axis, a period D apart, such that the phase shift in the quasiperiodicity of the elastodynamic field quantities is counterbalanced.

Using Eqs. (9), (10), and the elastodynamic reciprocity theorem leads to

$$\int_L [u_{\gamma\alpha}^g(\mathbf{x};\mathbf{x}') \tau_{\alpha\beta}^r(\mathbf{x}') - u_\alpha^r(\mathbf{x}') \tau_{\gamma\alpha\beta}^g(\mathbf{x};\mathbf{x}')] n_\beta(\mathbf{x}')\, ds(\mathbf{x}') = \{0, \tfrac{1}{2}, 1\} u_\gamma^r(\mathbf{x}) \quad \text{when } \mathbf{x} \in \{S^-, L, S^+\} , \tag{11}$$

where, if necessary, a Cauchy principal value of the relevant integral has been understood.

When $\mathbf{x} \in S^+$, Eq. (11) is an integral representation for the particle displacement of the reflected field. On account of the boundary condition on L, however, we prefer an integral representation with $\tau_{\alpha\beta} n_\beta$ instead of $\tau_{\alpha\beta}^r n_\beta$ in the integrand. The latter is obtained by apply-

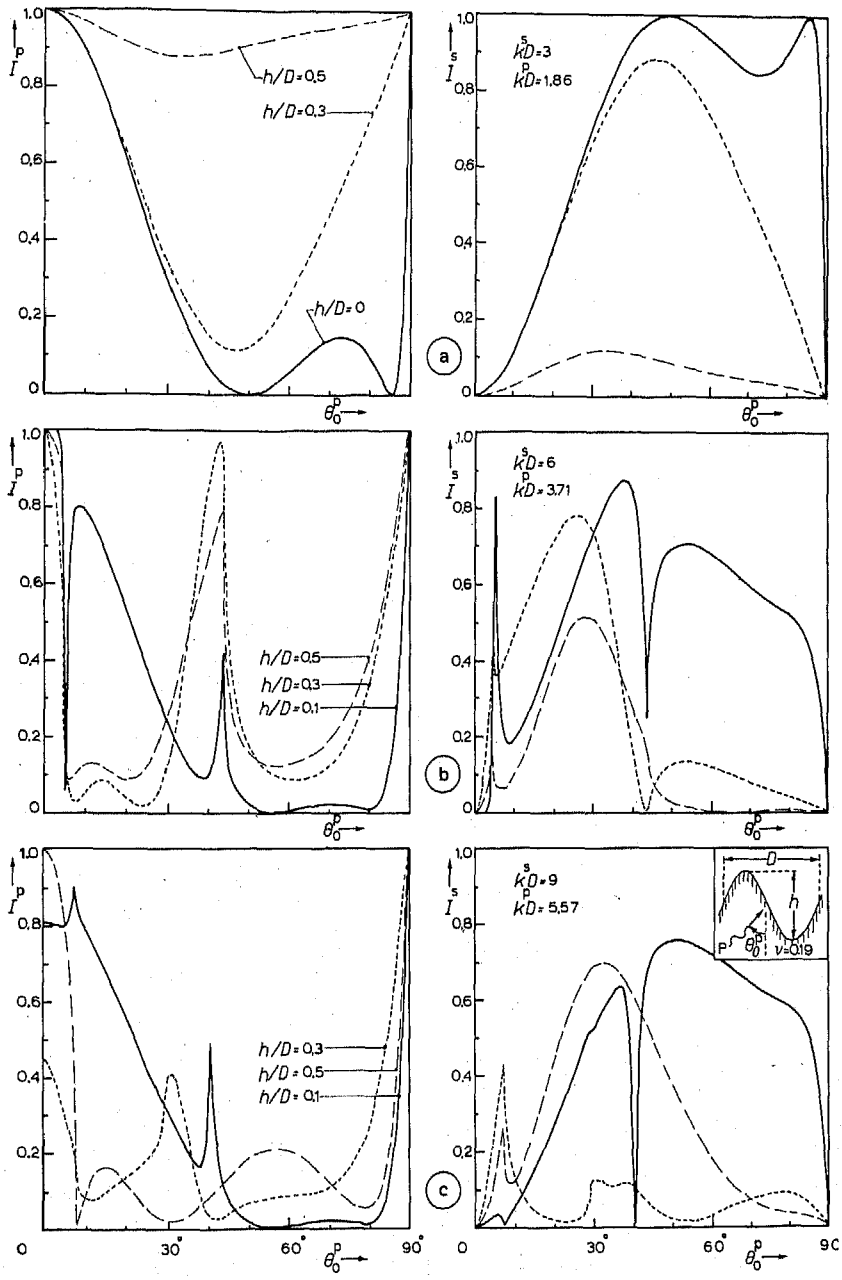

FIG. 3. The normalized intensities in the x_2 direction of zero spectral order I^p and I^s [see Eq. (19)] as a function of the angle of incidence θ_0^p for a sinusoidal profile with a Poisson ratio $\nu=0.19$, for an incident P wave; (a) $k^sD=3$, (b) $k^sD=6$, and (c) $k^sD=9$.

ing the elastodynamic representation theorem to the domain S^-, shown in Fig. 1, and the incident field.

We then obtain

$$\int_L [u^g_{\gamma\alpha}(\mathbf{x};\mathbf{x}')\tau^i_{\alpha\beta}(\mathbf{x}') - u^i_\alpha(\mathbf{x}')\tau^g_{\gamma\alpha\beta}(\mathbf{x};\mathbf{x}')]n_\beta(\mathbf{x}')\,ds(\mathbf{x}')$$
$$= -\{1, \tfrac{1}{2}, 0\}u^i_\gamma(\mathbf{x}) \quad \text{when } \mathbf{x}\in\{S^-, L, S^+\}\,. \tag{12}$$

Addition of Eqs. (11) and (12) and using Eqs. (6) and (7) yields

$$\int_L u_\alpha(\mathbf{x}')\tau^g_{\gamma\alpha\beta}(\mathbf{x};\mathbf{x}')n_\beta(\mathbf{x}')\,ds(\mathbf{x}')$$
$$= [u^i_\gamma(\mathbf{x}), -\tfrac{1}{2}u_\gamma(\mathbf{x}) + u^i_\gamma(\mathbf{x}), -u^r_\gamma(\mathbf{x})] \tag{13}$$

when $\mathbf{x}\in\{S^-, L, S^+\}$. From Eqs. (8), (9), (10), and (13) when $\mathbf{x}\in S^+$, and noting that $\tau^g_{\gamma\alpha\beta}$ consists of a superposition of P and SV waves, we obtain the following expressions for the reflection factors R^p_m and R^s_m:

$$R^p_m = \frac{ik^{p2}}{2\rho\omega^2 k^p_{2,m} D}\int_L u_\alpha(\mathbf{x}')T^p_{\alpha\beta,m}n_\beta(\mathbf{x}')\exp(-i\mathbf{k}^p_m\cdot\mathbf{x}')\,ds(\mathbf{x}'),$$
$$R^s_m = \frac{ik^{s2}}{2\rho\omega^2 k^s_{2,m} D}\int_L u_\alpha(\mathbf{x}')T^s_{\alpha\beta,m}n_\beta(\mathbf{x}')\exp(-i\mathbf{k}^s_m\cdot\mathbf{x}')\,ds(\mathbf{x}'), \tag{14}$$

in which we use for $T^p_{\alpha\beta,m}$ and $T^s_{\alpha\beta,m}$ the same expressions as the ones pertaining to the incident field listed in Table I, but with replacement of $\mathbf{k}^p$ and $\mathbf{k}^s$ by $\mathbf{k}^p_m$ and $\mathbf{k}^s_m$, respectively.

The expressions in (14) show that R^p_m and R^s_m can be calculated as soon as u_α on L is known.

This as yet unknown vector function is determined from Eq. (13) when $\mathbf{x}\in L$; which represents a vectorial integral equation of the second kind for u_α on L.

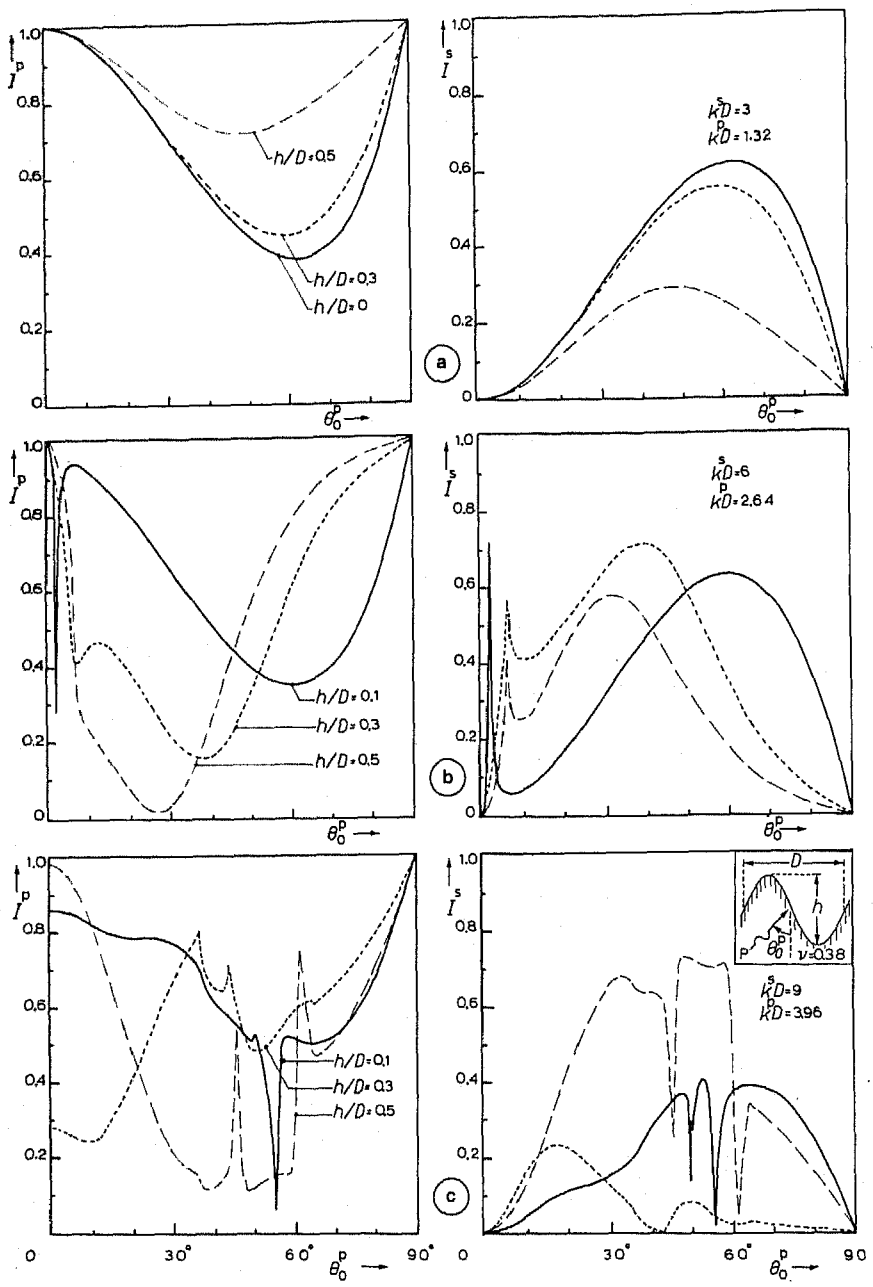

FIG. 4. The normalized intensities in the x_2 direction of zero spectral order I^p and I^s [see Eq. (19)] as a function of the angle of incidence θ_0^p for a sinusoidal profile with a Poisson ratio $\nu = 0.38$, for an incident P wave; (a) $k^sD = 3$, (b) $k^sD = 6$, and (c) $k^sD = 9$.

II. NUMERICAL RESULTS

So far, the method explained in the preceding section applies to the elastodynamic diffraction by a periodic boundary of arbitrary profile. In the present section, we report about the computations that have been performed for the sinusoidal boundary $x_2 = (h/2)\sin(2\pi x_1/D)$, in which h is the distance from top to valley (Fig. 3). For this type of boundary, a numerical solution of the integral equation based upon the method of cubic-spline approximation with point matching is to be preferred (cf. Refs. 2 and 5).

In this method the integration interval is subdivided by a mesh of points. The unknown components of the particle displacement are each approximated by a cubic spline (i.e., a polynomial of the third degree on each subinterval, continuous together with its first- and second-order derivatives at the chosen mesh points of the integration interval). As a result, the integral equation is replaced by a system of linear algebraic equations. The integrals in the relevant matrix elements are computed using the trapezoidal rule with two integration points between two successive mesh points of the chosen cubic-spline approximation. The series representation of the Green's tensor $\tau^{g}_{\gamma\alpha\beta}$ is truncated, in combination with a technique for accelerating the convergence.

As first test we verify the power relation

$$\sum_{\text{propagating P waves}} c_p |R_m^p|^2 \cos(\theta_m^p) + \sum_{\text{propagating SV waves}} c_s |R_m^s|^2 \cos(\theta_m^s) = \begin{cases} c_p \cos(\theta_0^p), & \text{for an incident P wave} \\ c_s \cos(\theta_0^s), & \text{for an incident SV wave.} \end{cases} \tag{15}$$

A second test makes use of the reciprocity relation for propagating waves, in which we distinguish two

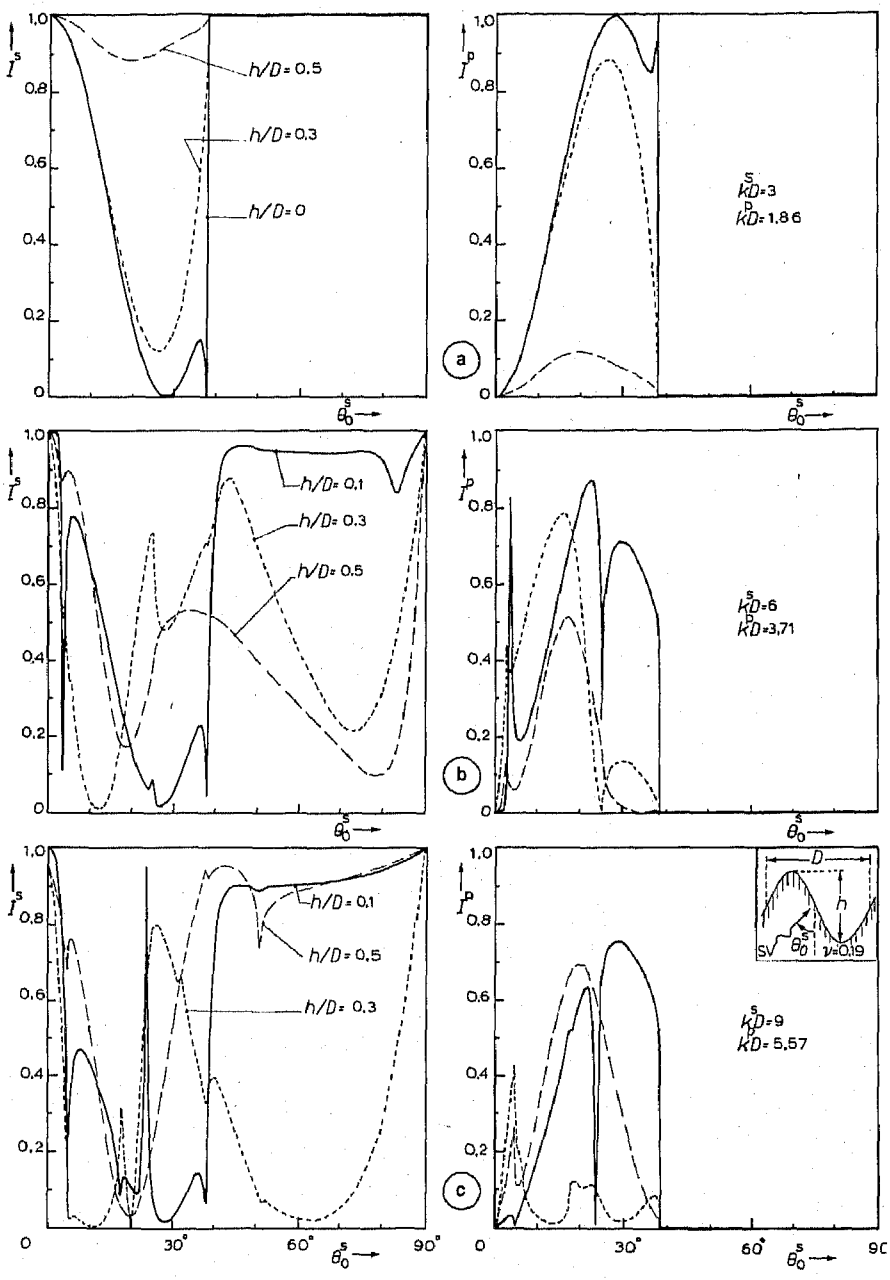

FIG. 5. The normalized intensities in the x_2 direction of zero spectral order I^s and I^p [see Eq. (20)] as a function of the angle of incidence θ_0^s for a sinusoidal profile with a Poisson ratio $\nu = 0.19$, for an incident SV wave; (a) $k^sD = 3$, (b) $k^sD = 6$, and (c) $k^sD = 9$.

cases (a) and (b). Case (a) refers to an incident wave and case (b) refers to an incident wave with a direction of propagation opposite to the reflected wave of the spectral order m of case (a). Then we can write

$$c_p R_m^{p,a} \cos(\theta_m^{p,a}) = c_s R_m^{s,b} \cos(\theta_m^{s,b}) ,$$

with case (a): incident SV wave,
case (b): incident P wave, (16)

$$R_m^{p,a} \cos(\theta_m^{p,a}) = R_m^{p,b} \cos(\theta_m^{p,b}) ,$$

with case (a): incident P wave,
case (b): incident P wave, (17)

$$R_m^{s,a} \cos(\theta_m^{s,a}) = R_m^{s,b} \cos(\theta_m^{s,b}) ,$$

with case (a): incident SV wave,
case (b): incident SV wave. (18)

The numerical results are presented for two different values of the Poisson ratio, viz., $\nu = 0.19$ and $\nu = 0.38$. For each of them three different values of h/D, viz., $h/D = 0.1$, 0.3, and 0.5 are investigated for both an incident P wave and an incident SV wave. The values pertaining to a plane boundary ($h/D = 0$) are presented for comparison. In Figs. 3–6 the normalized intensities in the x_2 direction of zero spectral order I^s and I^p are plotted as a function of the angle of incidence. The normalized intensity in the x_2 direction of zero spectral order is obtained by dividing the intensity of the reflected field of zero spectral order in the x_2 direction by the intensity of the incident field in the x_2 direction.

Hence

$$I^p = |R_0^p|^2 ,$$

$$I^s = [c_s \cos(\theta_0^s)/c_p \cos(\theta_0^p)]\,|R_0^s|^2 , \quad (19)$$

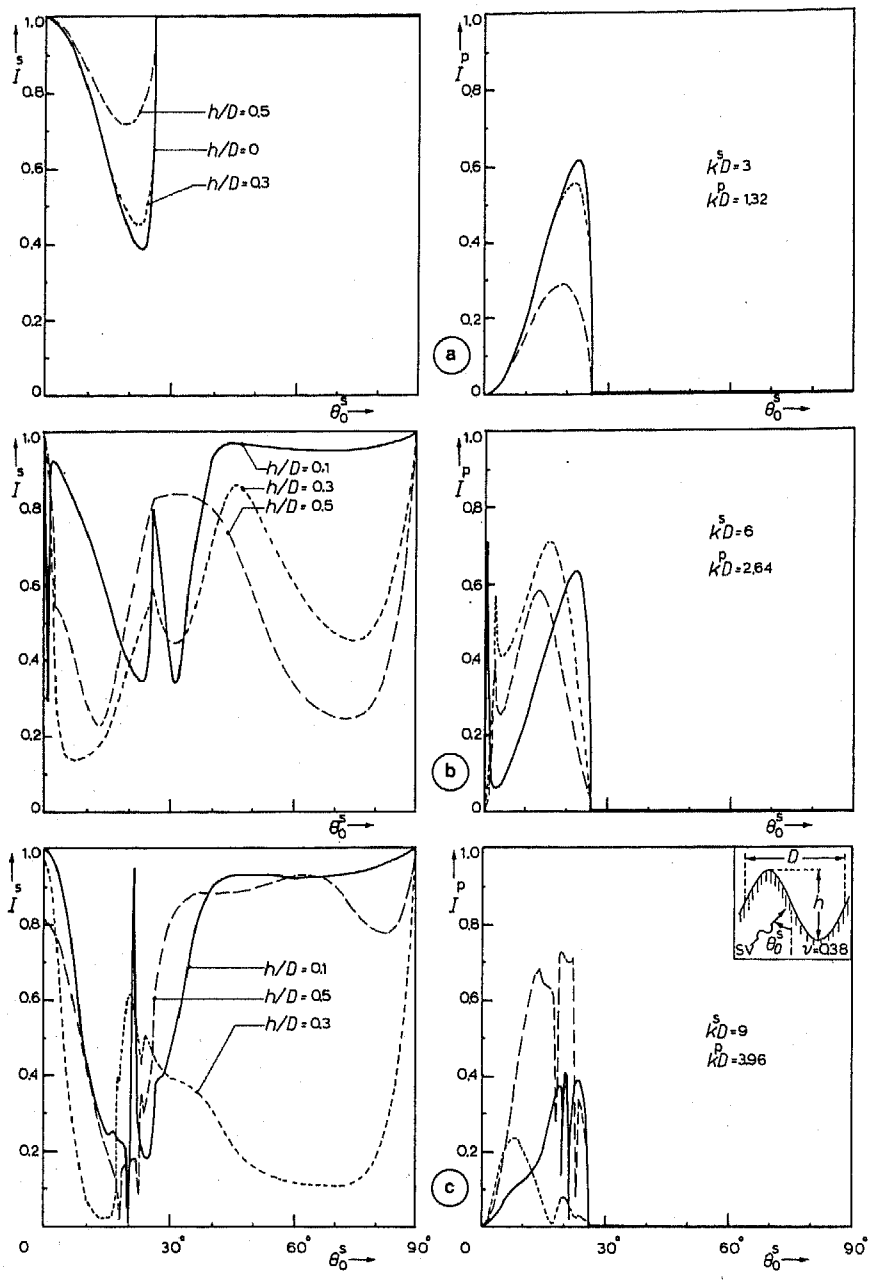

FIG. 6. The normalized intensities in the x_2 direction of zero spectral order I^s and I^p [see Eq. (20)] as a function of the angle of incidence θ_0^s for a sinusoidal profile with a Poisson ratio $\nu=0.38$, for an incident SV wave; (a) $k^sD=3$, (b) $k^sD=6$, and (c) $k^sD=9$.

for an incident P wave, and

$$I^s=|R_0^s|^2,$$
$$I^p=[c_p\cos(\theta_0^p)/c_s\cos(\theta_0^s)]|R_0^p|^2, \tag{20}$$

for an incident SV wave.

Figures 3 and 5 show the results pertaining to a Poisson ratio $\nu=0.19$ characterized by $k^sD=3$, 6, and 9 with $k^pD=1.86$, 3.71, and 5.57 for an incident P wave and an incident SV wave, respectively. Figures 4 and 6 show the results pertaining to a Poisson ratio $\nu=0.38$ characterized by $k^sD=3$, 6, and 9 with $k^pD=1.32$, 2.64, and 3.96 for an incident P wave and an incident SV wave, respectively.

In Table III the angles of incidence are listed for which the x_1 component of the wave vector of the reflected field of spectral order m, $k_{1,m}$, coincides with k^R, the x_1 component of the wave vector of Rayleigh waves along a plane, stress-free boundary. The latter follows from k^s and k^p.[6]

TABLE III. The angle of incidence (inc) in degrees at $k_{1,m}=k^R$ (k^R = wave number of Rayleigh waves along a plane, stress-free boundary).

	$k^sD=6$ $k^pD=3.71$ $k^RD=6.6$		$k^sD=9$ $k^pD=5.57$ $k^RD=9.9$		$k^sD=6$ $k^pD=2.64$ $k^RD=6.39$		$k^sD=9$ $k^pD=3.96$ $k^RD=9.58$	
	inc P	inc SV	inc P	inc SV	inc P	inc SV	inc P	inc SV
$m=1$	4.9	3	40.5	23.7	2.3	2	56.4	21.5
$m=-2$			28.6	17.2			48.9	19.4

TABLE IV. The intervals of the angles of incidence in degrees, in which the reflected wave of spectral order m is propagating for a Poisson ratio $\nu = 0.19$. The angle of incidence varies between 0° and 90°.

	$k^sD = 3$ $k^pD = 1.86$				$k^sD = 6$ $k^pD = 3.71$				$k^sD = 9$ $k^pD = 5.57$			
Spectral order	inc P		inc SV		inc P		inc SV		inc P		inc SV	
m	refl P	refl SV	refl SV	refl P	refl P	refl SV	refl SV	refl P	refl P	refl SV	refl SV	refl P
−2										39.8°–90°	23.3°–90°	51°–90°
−1					43.8°–90°	4.4°–90°	2.7°–90°	25.4°–90°	7.4°–90°	0°–90°	0°–90°	4.6°–90°
0	0°–90°	0°–90°	0°–90°	0°–38.2°	0°–90°	0°–90°	0°–90°	0°–38.2°	0°–90°	0°–90°	0°–90°	0°–38.2°
1										0°–29.2°	0°–17.6°	

TABLE V. The intervals of the angles of incidence in degrees, in which the reflected wave of spectral order m is propagating for a Poisson ratio $\nu = 0.38$. The angle of incidence varies between 0° and 90°.

	$k^s = 3$ $k^pD = 1.32$				$k^sD = 6$ $k^pD = 2.64$				$k^sD = 9$ $k^pD = 3.96$			
Spectral order	inc P		inc SV		inc P		inc SV		inc P		inc SV	
m	refl P	refl SV	refl SV	refl P	refl P	refl SV	refl SV	refl P	refl P	refl SV	refl SV	refl P
−2										64.2°–90°	23.3°–90°	73°–90°
−1						6.2°–90°	2.7°–90°	37.4°–90°	35.9°–90°	0°–90°	0°–90°	15°–90°
0	0°–90°	0°–90°	0°–90°	0°–26.1°	0°–90°	0°–90°	0°–90°	0°–26.1°	0°–90°	0°–90°	0°–90°	0°–26.1°
1										0°–43.3°	0°–17.6°	

From the figures we first conclude that anomalies in the intensity curves appear when $k_{1,m} = k^R$ and $h/D = 0.1$. Especially when $k_{1,1} = k^R$ the effect is most pronounced and decreases at greater values of h/D.

The anomalies at other values of the angle of incidence are due to the effect that a reflected wave of spectral order m change from propagating to evanescent or vice versa. For reference, the corresponding data are listed in Tables IV and V (for the Poisson ratios $\nu = 0.19$ and $\nu = 0.38$, respectively). This effect is the more pronounced the greater the depths of the grooves. Further we notice that the intensity curves of I^s in Fig. 3 and the intensity curves of I^p in Fig. 5 are of equal shape, but on a different scale. The same analogy we observe for I^s from Fig. 4 and I^p from Fig. 6. This also directly follows from the reciprocity relation (16) in conjunction with the symmetry of the geometry. Since in the configuration of Figs. 3(a), 4(a), 5(a), and 6(a) only the zero spectral orders are propagating, the energy conservation [Eq. (15)] follows directly from these figures. Further we remark that in Figs. 5(a) and 6(a) a cutoff occurs beyond a certain angle of incidence; this is a consequence of the fact that in this range we have no propagating P wave of zero spectral order.

The computations have been performed on the IBM 370/158 of the Computing Center of the Delft University of Technology. The computing time to calculate the quantities I^s and I^p for a single value of the angle of incidence is 8, 14, and 19 sec for $h/D = 0.1$, 0.3, and 0.5, respectively, when $k^sD = 9$.

We have found that round-off errors are not significant. It turned out that the error is due to the numerical discretization of the integral equation, the numerical evaluation of the integrals in the matrix elements, and the truncation of the series representation of the Green's tensor. An estimate of these errors has been made by increasing the number of linear equations (to approximate the integral equation), the number of integration points to evaluate the integrals in the matrix elements, and the number of terms to represent the Green's tensor. The estimated accuracy is then better than one percent.

The intensities of the plane boundary have been calculated with the aid of the formulas given in Ref. 6.

ACKNOWLEDGMENTS

The authors wish to thank A. T. de Hoop for his suggestions and remarks. The financial support of the Netherlands organization for the advancement of pure research (Z.W.O.) is gratefully acknowledged.

[1] B. A. Lippmann, "Variational formulation of a grating problem," J. Opt. Soc. Am. 43, 408 (1953).
[2] P. M. van den Berg, Appl. Sci. Res. 24, 261–293 (1971).
[3] A. T. de Hoop, "Representation Theorems for the Displacement in an Elastic Solid and Their Application to Elastodynamic Diffraction Theory," Ph.D. dissertation (Delft University of Technology, 1958) (unpublished).
[4] T. H. Tan, Appl. Sci. Res. 31, 29–52 (1975).
[5] J. H. Ahlberg, E. N. Nilson, and J. L. Walsh, *The Theory of Splines and Their Applications* (Academic, New York, London, 1967).
[6] J. D. Achenbach, *Wave Propagation in Elastic Solids* (North-Holland, Amsterdam, 1973), Chap. 5.